
Using the MCP1631 Family to Develop Low-Cost Battery Chargers

*Author: Terry Cleveland
Microchip Technology Inc.*

INTRODUCTION

As portable rechargeable applications continue to grow, there is an increase in demand for unique or custom battery charger designs. In addition to the increase in portable rechargeable applications, battery chemistry continues to improve and with that new charge methods and profiles are emerging. This all leads to the increase in demand for new or custom charge profile designs. In this application note, a mixed signal multi-chemistry battery charger design technique will be discussed that can accommodate the changing portable power management world.

The reliability and safety concerns with charging batteries can also benefit from programmable mixed signal designs. Charge rates and constant voltage levels can be updated in the field with a change in firmware. This allows the user to adapt to new smart battery packs and select desired runtime versus cycle life. By charging the battery to a lower constant voltage, the run time is shortened but the number of charge cycles will increase.

Another programmable battery charger feature is its ability to charge multi-chemistry battery packs. By detecting the number of cells and cell chemistry, a programmable charger can adapt to a new battery pack. This enables customers to choose between portability, runtime and cost when purchasing a portable system.

COMMON CHARGE PROFILES

NiMH Charge Profile

Figure 1 shows a typical charge profile for NiMH batteries. The charge cycle begins once a battery is detected by regulating a small current or conditioning current into the battery pack. If the cell voltage is above 0.9V per cell, it is safe to charge the pack with a fast charge or high current (for NiMH or NiCd, this current can range from 50% to over 100% of the batteries capacity). When the battery reaches capacity, cell manufactures recommend a top-off charge to complete the charge cycle. It is typically not recommended to trickle charge NiMH batteries, this can lead to overheating and reduced battery life. Fast charge termination for NiMH batteries can be tricky. As the battery reaches capacity, it no longer can accept a charge. The energy from the charger that was stored in the battery, now turns into heat causing the battery temperature to rise. There are two primary methods to determine when the battery has reached full charge, one is a sudden increase in temperature, the other being a subtle drop in battery voltage or $-dV/dt$. With NiMH batteries, the $-dV/dt$ can be difficult to detect, since the change can be very small, especially with lower charge rate designs. The $+dT/dt$ or temperature rise is typically easier to detect. For a robust design, both methods should be used so either can terminate the fast charge portion of the charge cycle. Once the fast charge is terminated, a timed top off charge is recommended, a continuous constant charge is not recommended for NiMH batteries.

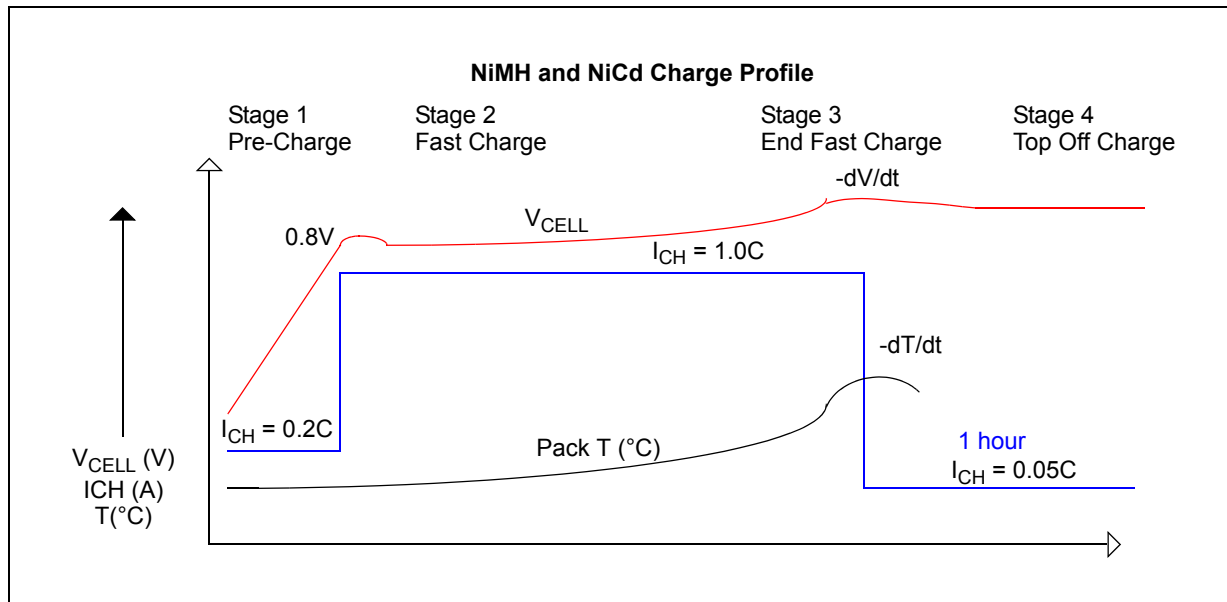


FIGURE 1: NiMH / NiCd Charge Profile.

Li-Ion Charge Profile

The charge profile for Li-Ion batteries starts with cell qualification. The cell voltage should be greater than 3.0V per cell before initiating a fast or high current charge. If the cell voltage is less than 3.0V per cell, a low value conditioning current is used to start the charge cycle. Once the cell voltage is above the 3.0V threshold, a fast charge or high current charge is initiated (0.5C to 1.0C). As the battery cell voltage rises, it reaches the maximum voltage value before it reaches full capacity. As an example, most Li-Ion batteries constant voltage level is 4.2V, where the battery charger now transitions into a constant voltage source (regulating voltage instead of current). The charge cycle continues as the charge current decreases while in the constant voltage mode. Once the charge current decreases to about 7% of the fast charge value, charge is terminated. Continuing the charge cycle past this point can damage the battery so the charge must be terminated. Once terminated a new charge cycle can be initiated when the battery voltage decreases to approximately 4.0V.

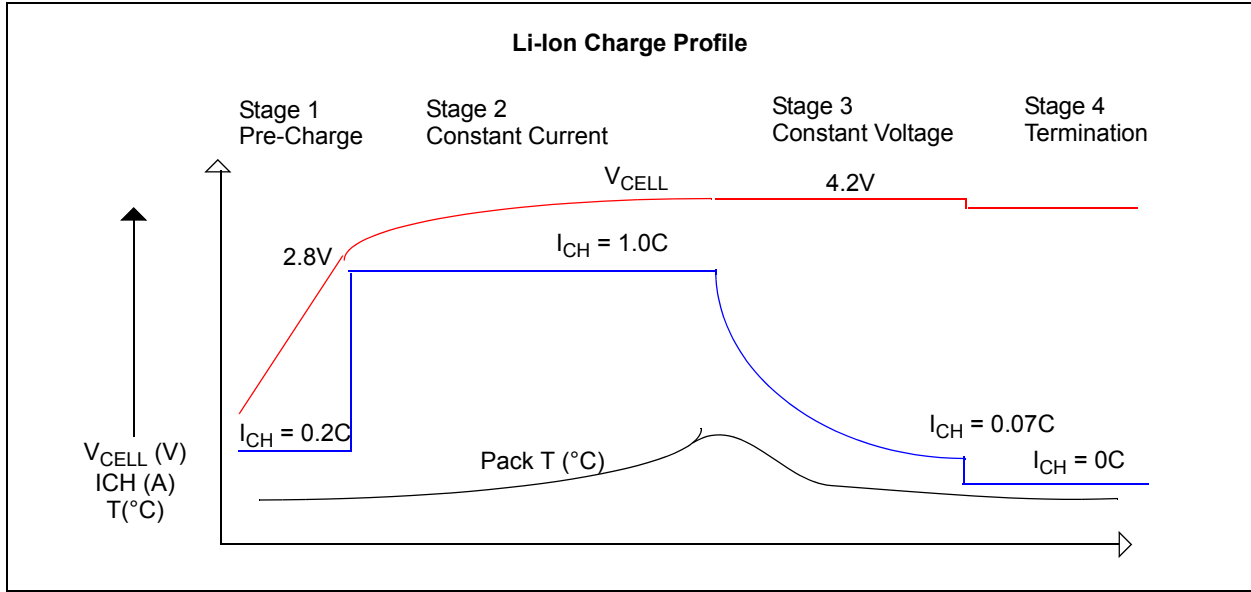


FIGURE 2: Li-Ion Charge Profile.

Multi-Chemistry Charger

There are significant differences in the charge profile between Ni batteries versus Li-Ion batteries. A multi-chemistry charger must be able to implement the proper profile and proper termination methods. This application note will demonstrate a charger that has the capability to charge single or multiple cells in series.

THE POWER BEHIND CHARGING BATTERIES

A battery charger and power supply have a lot in common, delivering a regulated output from a varying input. Two solutions are prevalent, linear and switch mode solutions. The linear solution is commonly used for low input voltage or low power applications. Its main drawback is internal power dissipation, calculated by the following formula:

$$P_{DISS} = (V_{IN} - V_{BATT}) \times I_{CHARGE}$$

For example, a +12V input linear charger would dissipate 18 watts when charging a +3.0V Li-Ion battery at 2A. Any power dissipation over a few watts is a challenge to cool.

Cooling 18 watts of power dissipation is no easy task, airflow and large heatsinks are required making a linear solution impractical.

$$P_{DISS} = P_{OUT} \times \left(\frac{1 - Eff}{Eff} \right)$$

A switching charger solution operating at similar conditions at 85% efficiency would dissipate approximately 1.05 Watts, making it much easier to cool. For high input voltage applications, switching battery chargers are smaller and more cost effective.

CHARGER POWER TOPOLOGY

Many switching regulator power topologies exist, buck, boost, SEPIC and flyback are all used to develop switching battery chargers (including others for very high power applications). A SEPIC converter is commonly used, it has advantages over buck and boost converters when used in battery charger applications.

- Capacitive Isolation:
 - There is no direct dc path from input to output providing isolation, this results in less power components and a safer battery charger.
- Primary Inductive Converter:
 - The SEPIC converter topology has an inductor at the input, smoothing input current reducing necessary filtering and generated source noise.
- Single Low Side Switch:
 - A single low side switch reduces MOSFET drive and current limit protection complexity.
- Buck-Boost Capability:
 - For applications where the input voltage can be above or below the battery voltage a SEPIC can buck or boost the input voltage.

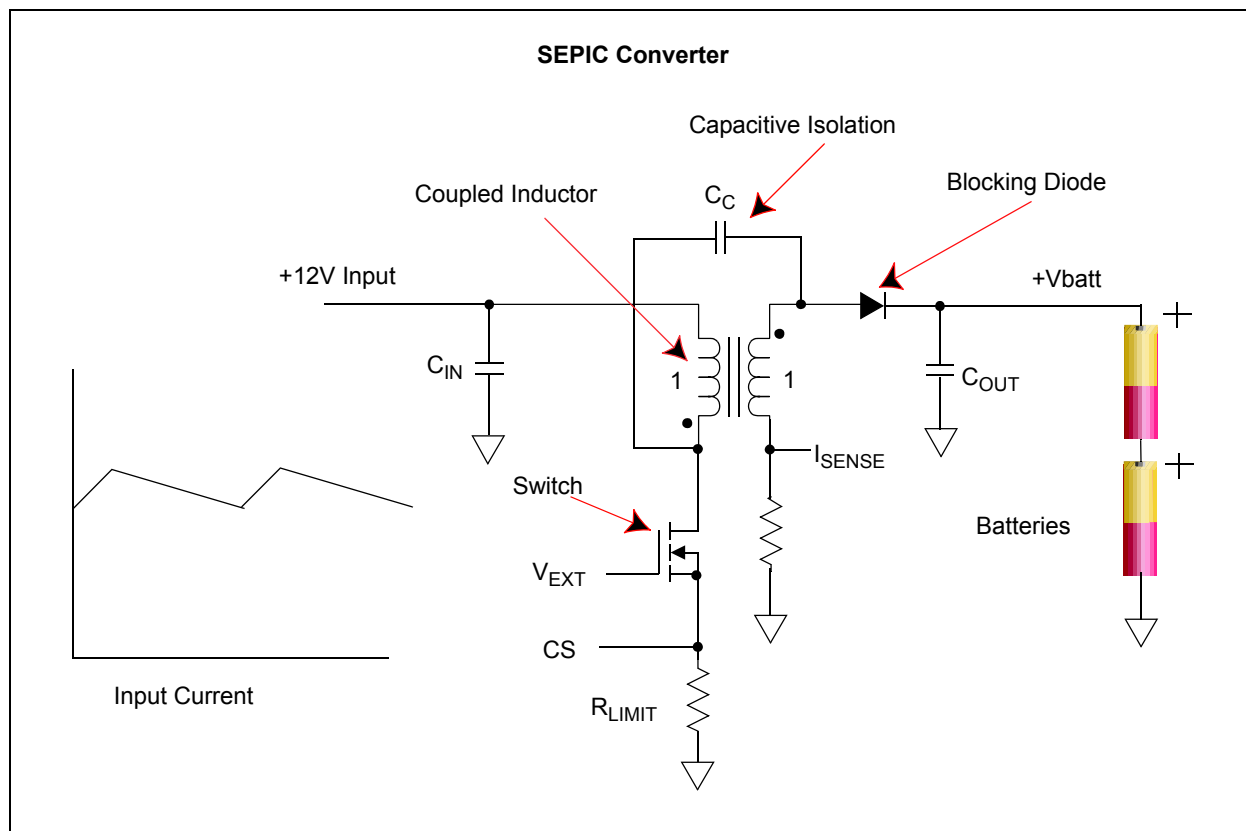


FIGURE 3: SEPIC Topology.

MULTI-CHEMISTRY BATTERY CHARGER DESIGN

The development of an intelligent multi-chemistry battery charger starts with the microcontroller. By implementing the charge algorithm in code, the charger can be adapted for multi-chemistry, custom charge profile and unique applications. For dc-dc converters, switching at high frequency with high performance gate drive capability, PWM control and high-speed protection, specialized analog circuitry is required. A new high-speed analog PWM, the MCP1631HV was developed for constant current SEPIC applications (battery chargers and LED drivers). By implementing the pulse width modulation, PWM, control using the

MCP1631, the battery charger has the benefits of analog speed and resolution. By controlling the charge algorithm using the microcontroller, the battery charger has the intelligence and flexibility to generate a profile for all battery types using digital timers and programmed algorithms.

As complex as this project sounds, it is really quite simple if the SEPIC converter is thought of as a microcontroller controlled current source. To increase current, the microcontroller simply increases the V_{REF} input to the MCP1631HV and to decrease current, the microcontroller decreases the V_{REF} input to the MCP1631HV. To generate a charge algorithm, the microcontroller measures the battery voltage using an

analog to digital converter(A/D), computes the desired charge current and adjusts the SEPIC controlled current source up or down.

To develop the charge algorithm for the NiMH battery, the microcontroller A/D converter is used to measure the battery pack voltage, when the pack voltage is within the desired range, the microcontroller sets the proper current level. To terminate the charge, two A/D inputs are used, one to sense the decreasing battery voltage and one to sense the increasing battery pack temperature. Charge termination will occur, if either one or both are detected.

To develop the algorithm for charging Li-Ion batteries, the A/D converter is used to measure pack voltage. Depending on pack voltage, the microcontroller will set the appropriate charge current. Once the pack voltage reaches the constant voltage phase, the A/D converter senses and regulates the pack voltage by adjusting the amount of current into the battery. The current continues to decrease until it reaches about 7% of the fast charge value. At this point, the microcontroller terminates the charge.

The MCP1631HV Implementation

The MCP1631HV integrates the necessary blocks to develop an intelligent, programmable battery charger or constant current source used for driving high power LED's.

INPUT VOLTAGE AND BIAS GENERATION

The MCP1631HV provides a regulated bias voltage for internal circuitry that is available for biasing the microcontroller and other components. It is available in two regulated voltage options, +5.0V and +3.3V and can handle a maximum output current of 250 mA. The maximum input voltage range for the regulator is +16.0V and can withstand transients to +18.0V. For regulated input voltages or higher input voltage applications, the MCP1631 device option without internal regulator can be used. By using a high voltage regulator to bias the MCP1631 and microcontroller, the range of input voltage for the design is only limited by the regulator maximum input and power train design.

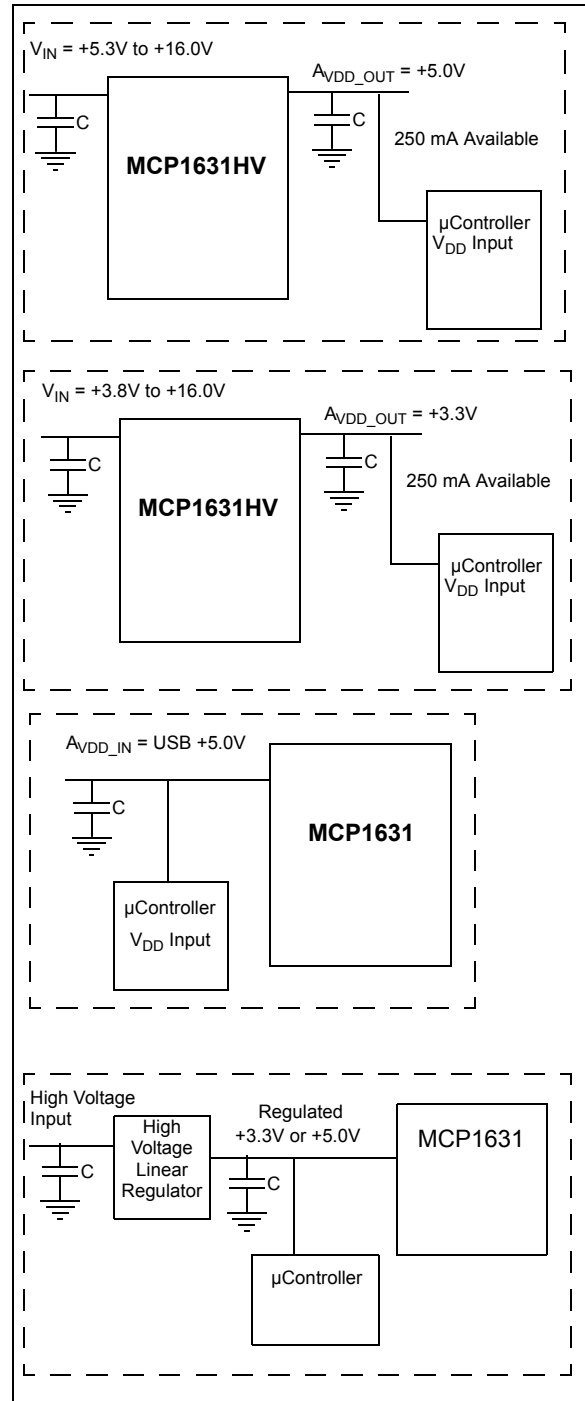


FIGURE 4: MCP1631HV and MCP1631 Bias Voltage Options.

AN1137

HIGH SPEED ANALOG PWM OPERATION

The high-speed analog PWM is used to control the power train switch ON and OFF times to regulate the output of the converter. Voltage or current can be regulated depending on what is being sensed. For the SEPIC Battery Charger application, the MCP1631HV is always regulating current, the microcontroller is programming this current.

The analog PWM starts with the oscillator input, typically a microcontroller PWM output or simple clock output (50% duty cycle). When the oscillator input is high, the V_{EXT} output is pulled low, (N-Channel MOSFET Driver is ON). A new cycle is started when the OSC_IN input transitions from a high to a low, the internal N-channel MOSFET driver turns off and the P-Channel MOSFET turns on driving the V_{EXT} pin high turning on the external N-Channel MOSFET. Current begins to ramp up in the external CS sense resistor until it reaches 1/3 of the level of the error amplifier output voltage (limited to 0.9V by error amplifier clamp). The 0.9V limit is used as an overcurrent limit, the

ramping current is used for peak current mode control CS signal. A filter is used on the CS input to remove the leading edge turn on spike associated with the turn on of the external power MOSFET. The driver P-Channel MOSFET is powered using a separate P_{VDD} pin helping to keep switching noise off of the A_{VDD} pin and sensitive CS circuitry.

The error amplifier is configured as an integrator, so any difference between its inputs, V_{REF} and V_{FB} are quickly removed. If the V_{FB} input is high, the inverting error amplifiers output, (COMP), will be pulled down, lowering the peak current into the switch and lowering duty cycle bringing the output back into regulation. The external R and C used for compensation is used to control the speed of the error amplifiers output response. If not compensated properly, the error amplifier output will move to fast (unstable system with under damped oscillations) or slow (over damped system with no performance or response to changes). The V_{REF} input is set by the microcontroller to program the proper charge current.

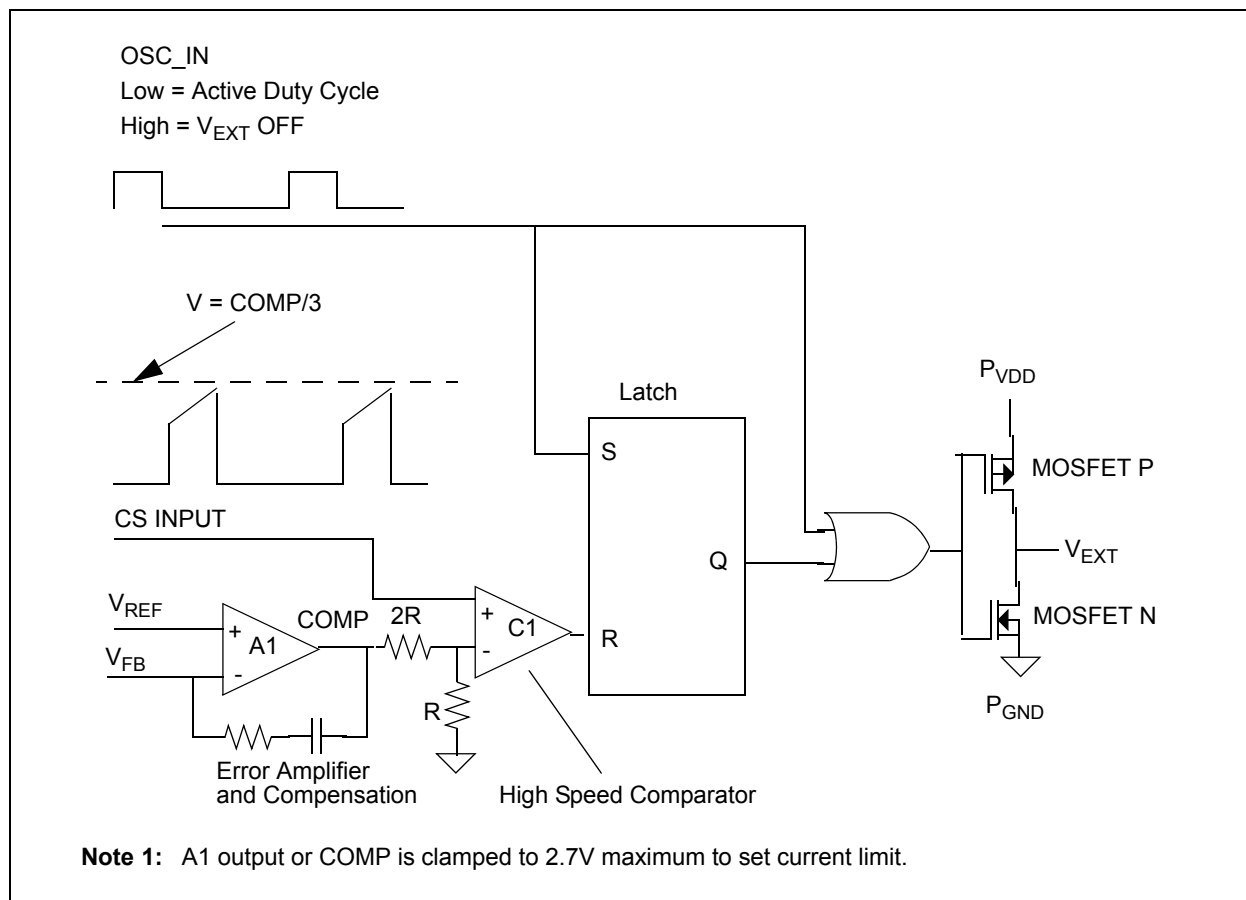


FIGURE 5: Analog PWM Operation.

CURRENT REGULATION

To sense battery current for regulation in a SEPIC converter, the secondary winding of the coupled inductor can be used. The average current flowing through the secondary winding is equal to the current flowing into the battery. As shown, this topology does not require the sense resistor in series with the battery, removing any power lost in series with the battery while running the system. When sensing battery current, a low value sense resistor is desired to minimize power loss, the

MCP1631HV integrates an inverting $10V/V$ gain amplifier to increase the battery current sense signal. The microcontroller sets the V_{REF} input to the desired current level, the MCP1631HV uses the V_{REF} input as a reference for regulation.

The resistor in series with the external SEPIC switch provides a high speed current limit protecting the switch and other power train components from a short circuit or over current condition.

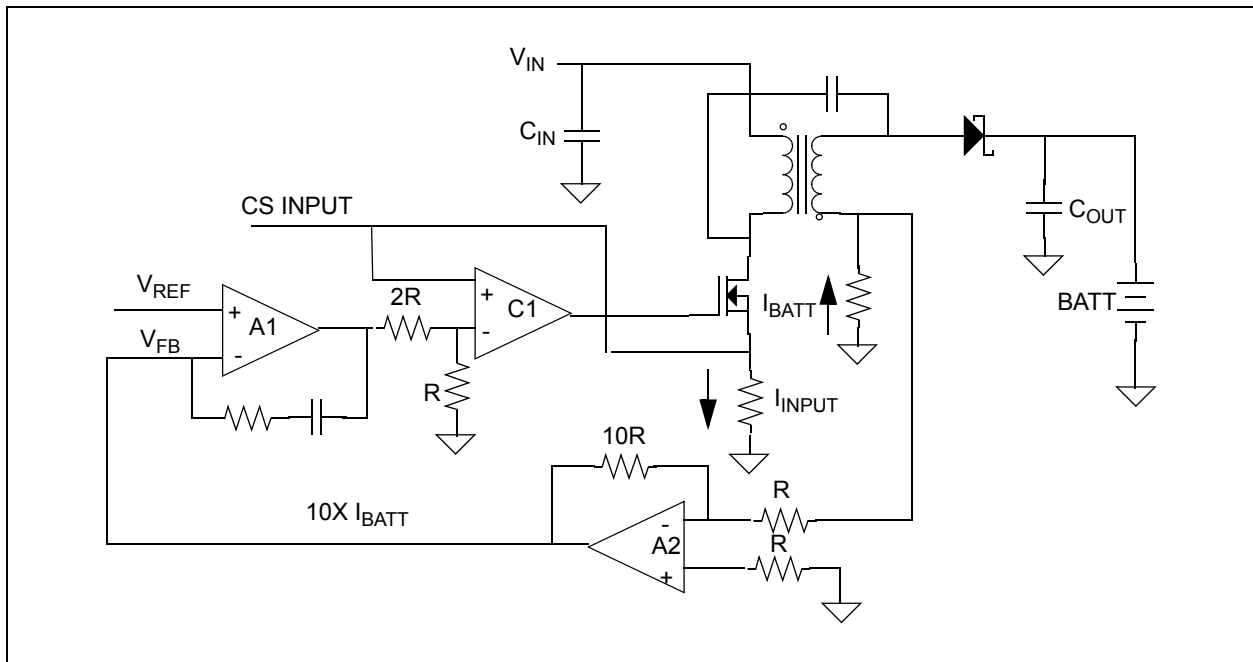


FIGURE 6: Current Regulation Diagram.

SENSING BATTERY VOLTAGE

Using the internal microcontroller A/D converter to sense battery voltage is a popular approach. An issue with this technique is the A/D converter requires a low source impedance to perform accurate readings. Low source impedance requires low resistance values that draw excessive quiescent current from the battery. The MCP1631HV integrates a low current amplifier (A3), configured as a unity gain buffer. The buffer output impedance is low, driving the SAR A/D converter, while consuming very little quiescent current. A high value resistor divider is used to drop the battery voltage to an acceptable range. R1, R2 and R3 values are selected to minimize the drain on the batteries, typically drawing on the order of $1 \mu A$. The microcontroller reads the A/D converter, calculates the current setting and adjusts the V_{REF} input to regulate current.

Overvoltage (OV) protection is a common battery charger protection feature. The OV protection is not there to protect the battery, it is used to protect the power train from excessive voltage if the battery is

removed or opens. OV protection is typically required for any current source application (battery chargers, LED drivers).

The MCP1631HV integrates an internal high speed OV comparator that has a $1.2V$ reference connected to its inverting input. If the voltage on the OV_IN pin exceeds the $1.2V$ threshold, the V_{EXT} output is asynchronously terminated. Switching will resume after the voltage has dropped more than the built in $50 mV$ of hysteresis. If a battery is removed during the charge cycle, the charger output voltage will be limited to a safe value.

AN1137

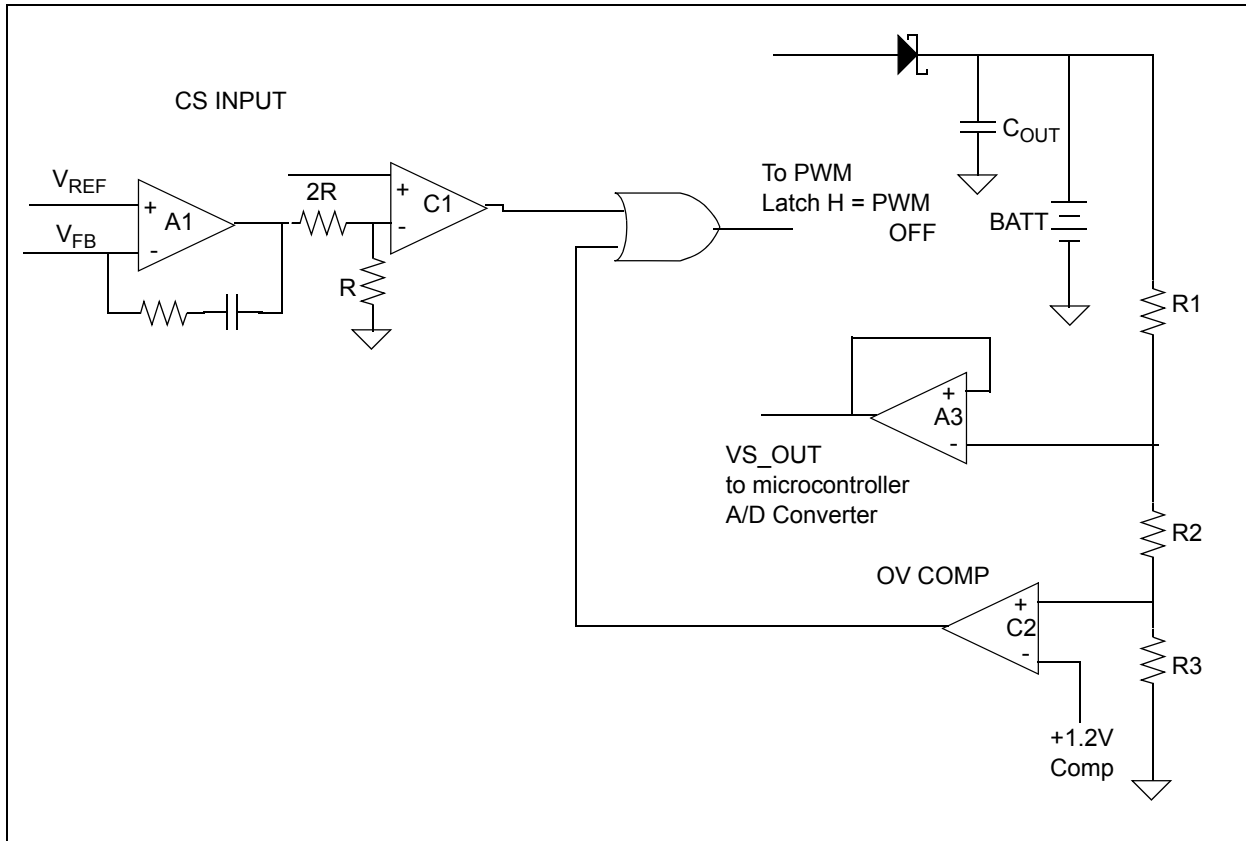


FIGURE 7: MCP1631HV Voltage Buffer and Overvoltage Comparator Setup.

AN1137

Charger Reference Board Design

charger application.

A battery charger reference design was developed for the MCP1631HV to evaluate the device in a battery

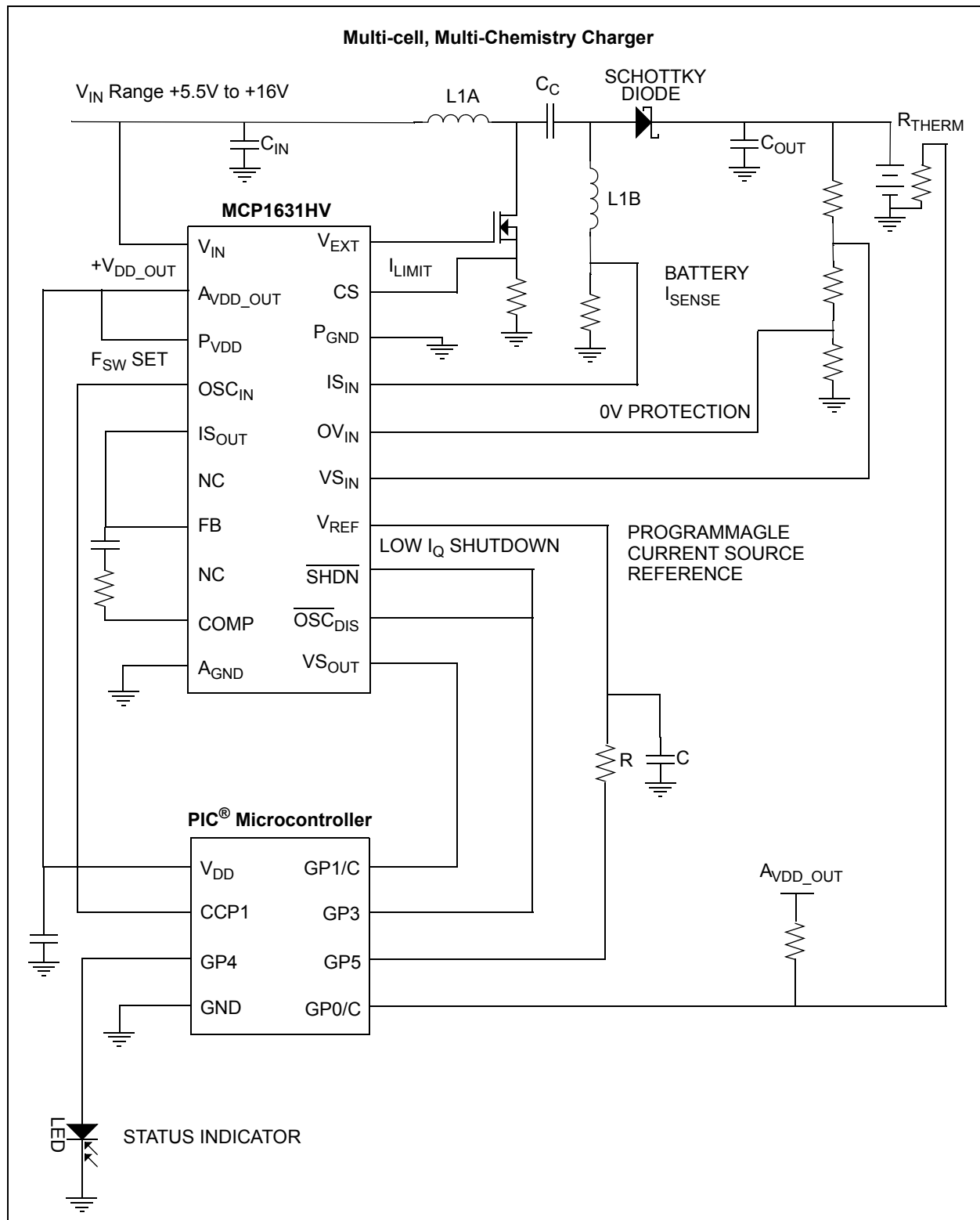


FIGURE 9: Charger Diagram.

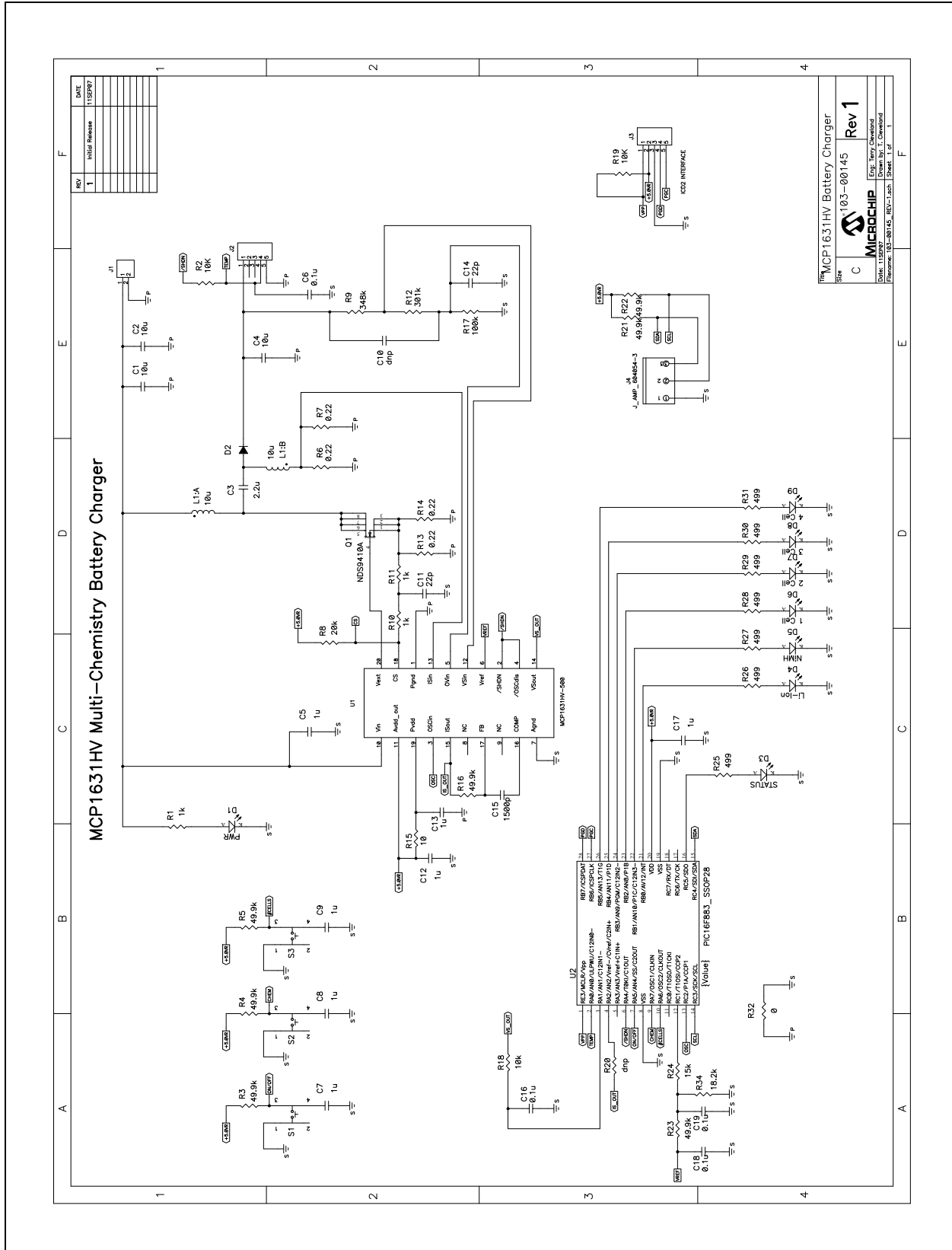


FIGURE 10: Detailed Schematic.

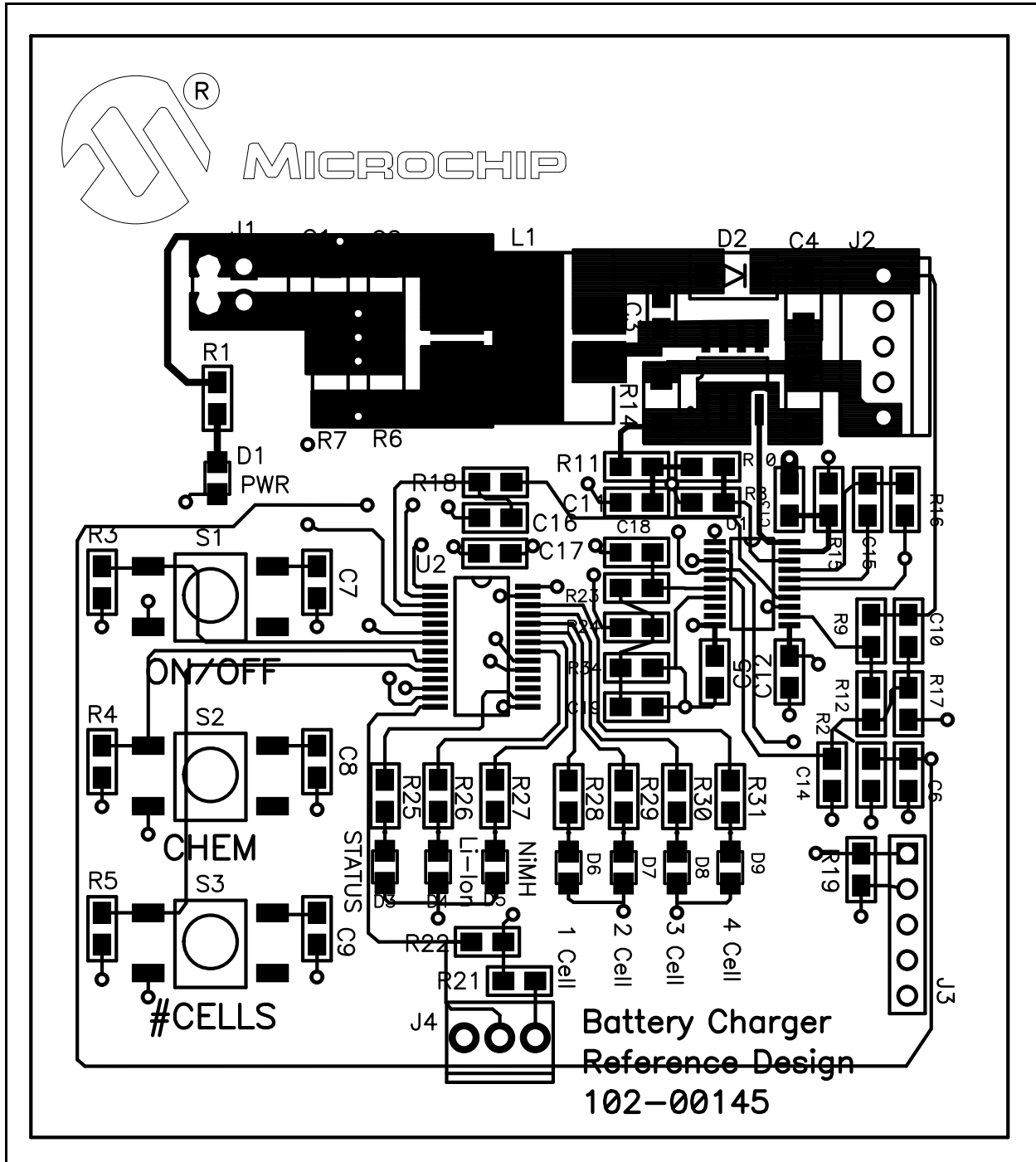


FIGURE 11: Board Layout.

THE DESIGN DETAILS OF CHARGING BATTERIES USING THE PIC[®] MICROCONTROLLER AND MCP1631HV WITH A SEPIC TOPOLOGY

Design Example:

- $V_{IN} = 12V$
- $V_{BATT} = 0V$ to $4.2V$
- $I_{BATT} = 200$ mA Pre-Charge Current
- $I_{BATT} = 2A$ Fast Charge Current
- $I_{BATT} = 140$ mA termination or “tail” current
- Overvoltage Protection

SEPIC Power Train Design

- Calculate Maximum Output Power

$$P_{OUT} = V_{BATT} \times I_{BATT}$$

$P_{OUT} = 4.2V \times 2.0A$ or 8.4 Watts

$$P_{IN} = \frac{P_{OUT}}{\text{Efficiency}}$$

- By making an efficiency estimate, the converter input power can be estimated. The typical efficiency of a SEPIC converter in this power range using a schottky diode for the output rectifier is around 85%.
- $P_{IN} = 8.4$ Watts / 0.85 or 9.88 Watts
- $I_{IN} = P_{IN} / V_{IN}$
 - $I_{IN} = +12V / 0.88$ Watts
 - $I_{IN} = 1.21$ A

With I_{IN} and I_{BATT} known, the average inductor current for each winding is known.

Inductor Ripple Current

For the coupled inductor, the effective inductance is twice the value of the inductor, this is a result of 2x the voltage across 2x the number of turns. Since the value of L is proportional to n^2 , the effective inductance is twice the actual value of the inductor.

$$\frac{2 \times V}{n^2}$$

A 10 μH inductor looks like a 20 μH inductor (for coupled inductors only). Larger inductance reduces ripple current and operates in the continuous mode at lighter loads, an advantage over non-coupled inductor solutions.

The input and output inductor ripple current is equal to:

$$\Delta I_L = \frac{V_L}{L} \times t_{ON}$$

Where T_{ON} is the amount of time the SEPIC switch is turned on:

$$t_{ON} = \text{DutyCycle} \times \frac{1}{F_{SW}}$$

Where Duty Cycle for a SEPIC converter operating in continuous conduction mode is equal to:

$$\text{DutyCycle} = \frac{V_{OUT}}{V_{OUT} + V_{IN}}$$

To derive the transfer function of the SEPIC converter, start by balancing the inductor volt-time product in the boost stage (W_1).

Q_1 Turned on (+ Slope):

$$\Delta I_{W1}/t_{ON} = V_{IN}/L_{W1}$$

Q_1 Turned off (- Slope):

$$\Delta I_{W1}/t_{OFF} = \frac{V_{C1} + V_{OUT} - V_{IN}}{L_{W1}}$$

Inductor slope's must be equal for volt-time balance:

$$t_{ON} \times \frac{V_{IN}}{L_{W1}} = t_{OFF} \times \frac{V_{C1} + V_{OUT} - V_{IN}}{L_{W1}}$$

Multiply both sides by $1/(t_{ON} + t_{OFF})$:

$$V_{IN} \times D = (V_{C1} + V_{OUT} - V_{IN}) \times (1 - D)$$

Solve for V_{C1} :

$$V_{C1} = V_{IN} \times \left(\frac{1}{1-D} \right) - V_{OUT}$$

For the second stage, the inductor slopes must also be equal.

Q_1 Turned on (+ Slope):

$$\frac{\Delta I_{W2}}{t_{ON}} = \frac{V_{C1}}{L_{W2}}$$

AN1137

Q₁ Turned off (- Slope):

$$\frac{\Delta I_{W2}}{t_{OFF}} = \frac{V_{OUT}}{L_{W2}}$$

Inductor slope's must me equal for volt-time balance:

$$t_{ON} \times \frac{V_{C1}}{L_{W2}} = t_{OFF} \times \frac{V_{OUT}}{L_{W2}}$$

Multiply both sides by 1/(t_{ON} + t_{OFF}):

$$V_{C1} \times D = V_{OUT} \times (1 - D)$$

Solving for V_{C1}.

$$V_{C1} = V_{OUT} \times \left(\frac{1-D}{D} \right)$$

Set V_{C1} = V_{C1} for both the Boost stage and the Buck-Boost stage:

$$V_{C1} = V_{IN} \times \left(\frac{1}{1-D} \right) - V_{OUT} = V_{OUT} \times \left(\frac{1-D}{D} \right)$$

Solving for V_{OUT}/V_{IN}:

$$\frac{V_{OUT}}{V_{IN}} = \left(\frac{D}{1-D} \right)$$

Looking back, if D/(1-D) × V_{IN} is substituted for V_{OUT}, it is shown that V_{C1} = V_{IN}. This is true, if C₁ is large enough that the ripple voltage on C₁ is low.

Now that the duty cycle is known as a V_{OUT}/V_{IN} relationship, the duty cycle can be calculated for any input output condition. Remember, this transfer function is dependent upon the fact that inductor current is continuous or never reached zero. If it does reach zero, this transfer function is no longer true and there is another state added to the operation.

Power Train Design

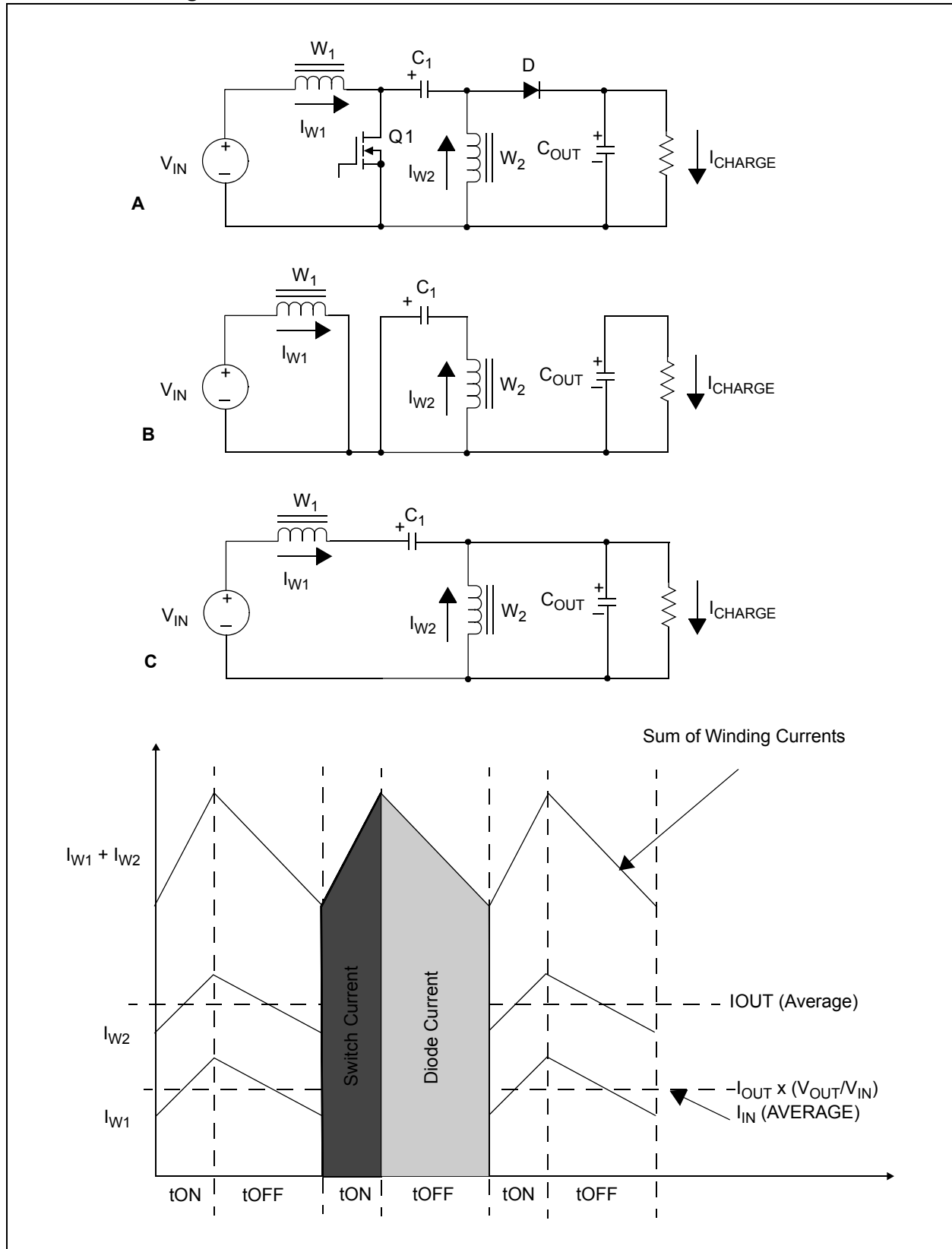


FIGURE 12: SEPIC Converter Inductor, Switch and Diode Currents.

AN1137

Inductor Winding Current Calculation

The first step to calculating the inductor winding current is to know the maximum output power. For this constant current battery charger application, the output power is simply the maximum output voltage times the charge current.

$$P_{OUT} = V_{OUT} \times I_{CHARGE}$$

Maximum output voltage is equal to 4.2V (1 battery @ 4.2V).

$$P_{OUT} = 4.2V \times 2 \text{ A or } 8.4 \text{ Watts.}$$

Since energy is conserved, the input power is equal to the output power (assuming 100% efficiency). An efficiency estimate can be used to closer approximate the input current.

$$P_{IN} = P_{OUT} / (\text{Efficiency})$$

Where:

$$P_{IN} = 8.4 \text{ Watts} / 85\%; \text{ 85\% used as a typical efficiency estimate}$$

$$P_{IN} = 9.88 \text{ Watts}$$

The average input current is equal to the input power divided by the input voltage:

$$I_{IN(AVG)} = P_{IN} / V_{IN}$$

Where:

$$I_{INAVG} = 9.88 \text{ Watts} / 12V \text{ (Nominal)}$$

$$I_{INAVG} = 824 \text{ mA. (Typical average input current)}$$

The peak-to-peak W_1 inductor current ripple calculation was shown earlier. Given the derived transfer function and the maximum voltage on the output of the converter to be 4.2V, the switch on time is estimated.

Switch On Time:

$$t_{ON} = \frac{V_{OUT} / (V_{OUT} + V_{IN})}{F_{SW}}$$

For the 12V input and 4.2V output case, the switch ON time is estimated to be approximately 519 ns. (500 kHz switching frequency).

The input peak-to-peak ripple current can be calculated:.

GIVEN: $L_{W1} = L_{W2} = 20 \mu\text{H}$ (10 μH Coupled)

Input Peak-to-Peak Ripple Current (W_1)

$$\Delta I_{L(W1)} = (12V / 20 \mu\text{H}) \times t_{ON} = 311 \text{ mA}$$

$$I_{L(W1)PK} = I_{INAVG} + 1/2 \times \Delta I_{L(W1)}$$

$$I_{L(W1)PK} = 980 \text{ mA for winding 1 (} W_1)$$

$$I_{L(W1)MIN} = I_{INAVG} - 1/2 \times \Delta I_{L(W1)}$$

$$I_{L(W1)MIN} = 669 \text{ mA for winding 1 (} W_1)$$

The ripple current in winding (W_2) is calculated in a similar fashion. The main difference is that the average current in W_2 is equal to I_{OUT} or 2A in this application.

W_2 Peak-to-Peak Ripple Current

$$\Delta I_{L(W2)} = (12V / 20 \mu\text{H}) \times t_{ON} = 311 \text{ mA}$$

$$I_{L(W2)PK} = I_{OUTAVG} + 1/2 \times \Delta I_{L(W2)}$$

$$I_{L(W2)PK} = 2.16 \text{ A for winding 2 (} W_2)$$

$$I_{L(W2)MIN} = I_{OUTAVG} - 1/2 \times \Delta I_{L(W2)}$$

$$I_{L(W2)MIN} = 1.85 \text{ A for winding 1 (} W_2)$$

Note: In the case of $V_{IN} = V_{OUT}$, the current in $W_1 = W_2$ (ripple and average).

The coupled inductor winding currents calculated above are used to determine the size of the inductor necessary. High switching frequency has several advantages, smaller ripple current, lower peak and RMS current and lower volt-time product on the inductor core. This leads to a small, low-cost solution.

SEPIC Switch Current and Voltage Calculations

The switch current (I_{Q1}) is equal to the combination of the winding currents during the switch on time. When the switch is turned on, it conducts the current in W_1 and W_2 .

$$I_{SW} = I_{W1} + I_{W2} = 2.82A \text{ (Average)}$$

$$I_{SWPK} = 2.82A + 311 \text{ mA} = 3.14A$$

The minimum switch current is equal to:

$$I_{SWMIN} = 2.82A - 311 \text{ mA} = 2.51A$$

RMS of a Trapezoidal waveform

$$I_{SWRMS} = \sqrt{D \times \left(\frac{I_A^2 + I_A \times I_B + I_B^2}{3} \right)}$$

Where:

$$I_A = 2.51A = \text{Minimum,}$$

$$I_B = 3.14A = \text{Maximum}$$

The RMS value of the switch current is approximately 1.44 mA.

The peak switch voltage is equal to $V_{IN} + V_{OUT}$ for the SEPIC converter. Any leakage inductance voltage spike is clamped through the output diode by the output capacitor. A switch voltage rating for this application should be a minimum of $V_{IN(MAX)} + V_{OUT(MAX)}$.

$$V_{SW} = 12V + 4.2V$$

$$V_{SW} = 16.2V$$

A 30V, 30 milli-ohm, logic-level switch is selected. MOSFET switching losses should also be considered when selecting the MOSFET switch. Low on resistance switches tend to have high capacitance and will switch slower, increasing switching losses. The lowest $R_{DS(ON)}$ MOSFET is not necessarily the best choice. When using the SOIC-8 package for a 30V MOSFET, there are many choices available.

SEPIC Diode Voltage and Current Calculations

A schottky diode is recommended for low-voltage applications. For battery charger applications, the SEPIC diode will block current flow from the battery back to the input. The reverse leakage current of the selected schottky diode can be a critical parameter, if low battery drain is desired. Low schottky diode forward drop is also a key parameter; the low drop improves converter efficiency.

The maximum reverse voltage across the SEPIC diode occurs during the switch on time. The cathode of the schottky diode is connected to V_{OUT} , the anode of the schottky diode is connected to the SEPIC coupling capacitor. The voltage across the coupling capacitor voltage is equal to V_{IN} ; the voltage across the diode is equal to $V_{OUT} - (-V_{IN})$ or $V_{OUT} + V_{IN}$.

The peak SEPIC diode current occurs when the switch is turned off. The peak diode current is equal to the peak current in W_2 , plus the peak current in W_1 or 3.14A. The average diode current is equal to the output current (I_{OUT}), typical of all topologies with a series diode in the path of the output.

SEPIC Coupling Capacitor (C_1) RMS Current Calculations and Voltage Rating

The RMS current in the SEPIC coupling capacitor is mainly dependant upon output power with some influence by inductor ripple current. As output power increases, the capacitor ripple current will increase as well. As shown in Figure 12 (during the switch on time), the current in winding 2 (output current) is flowing through the coupling capacitor C_1 . During the switch off time, the C_1 current is equal to the current in winding number 1 (W_1). As previously discussed, the W_1 current is equal to the average input current. Therefore, the worst case or maximum RMS current in the coupling capacitor will occur at maximum output power

and minimum input voltage. To estimate size for the coupling capacitor, the capacitor derivative equation can be used.

$$I_C = C \times \frac{dV}{dt}$$

The rate of change of voltage across the capacitor is related to the amount of current through the capacitor and the size or energy storage capability of the capacitor.

For the SEPIC converter coupling capacitor, the voltage is approximated to be a DC value when deriving the duty cycle. The ripple voltage should be no more than 5% of the voltage across the capacitor or the input voltage. In this example, the input voltage and C_1 DC voltage is 12V, so there should be no more than 5% or 600 mV of ripple on the coupling capacitor.

In this example there is an average of 2A flowing through the coupling capacitor during the switch on time. The on time is approximately 26% or 520 ns. To keep the capacitor voltage ripple less than 5% of V_{IN} , or 600 mV, the amount of capacitance is equal to $(2A) / (600mV/520 \text{ ns})$ or 1.73 μF . For this application a standard value 2.2 μF X7R 25V rated ceramic capacitor should be used.

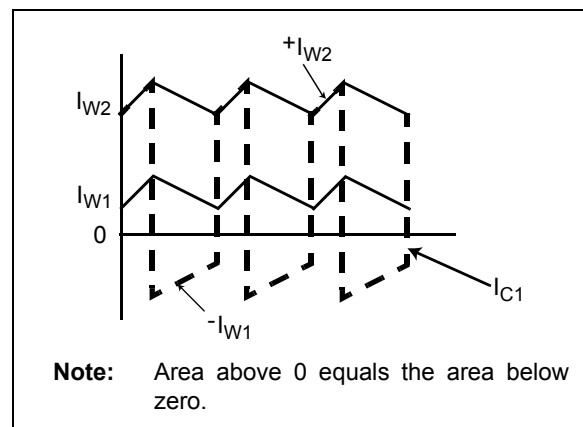


FIGURE 13: C_1 Ripple Current.

As shown in Figure 13, the coupling capacitor ripple current is largely dependent upon output power and input voltage. As the input voltage decreases, the current in W_1 increases. During the switch on time, the current flowing in W_2 is equal to the current flowing in C_1 . When the switch turns off, the current quickly changes magnitude and direction so that the current flowing in C_1 is equal to the current in W_1 , magnitude and direction.

As an approximation, the RMS current in C_1 :

$$I_{C1(RMS)} = I_{OUT} \times \sqrt{V_{OUT}/V_{IN}}$$

For worst-case situations, the RMS current in the C_1 coupling capacitor is equal to $2A \times (4.2V / 12V)^{1/2}$ or 1.18A. The current rating for small multi-layer ceramic capacitors is typically much higher than 1.18A. For higher power applications, it may be necessary to use multiple capacitors in parallel to keep the RMS current within ratings.

CONCLUSION

For applications that require intelligent power management solutions like battery chargers, the combination of a microcontroller and MCP1631 high-speed PWM is very powerful. It brings the programmability benefits of the microcontroller and adds the performance of a high-speed analog PWM. The analog PWM will respond to changes in input voltage and output current very quickly. No code or execution time is necessary to regulate or protect the circuit. The microcontroller is used for programmability, establishing charge profile conditions and monitoring the circuit for fault conditions and taking the appropriate action, in the event of a specific fault.

Note the following details of the code protection feature on Microchip devices:

- Microchip products meet the specification contained in their particular Microchip Data Sheet.
- Microchip believes that its family of products is one of the most secure families of its kind on the market today, when used in the intended manner and under normal conditions.
- There are dishonest and possibly illegal methods used to breach the code protection feature. All of these methods, to our knowledge, require using the Microchip products in a manner outside the operating specifications contained in Microchip's Data Sheets. Most likely, the person doing so is engaged in theft of intellectual property.
- Microchip is willing to work with the customer who is concerned about the integrity of their code.
- Neither Microchip nor any other semiconductor manufacturer can guarantee the security of their code. Code protection does not mean that we are guaranteeing the product as “unbreakable.”

Code protection is constantly evolving. We at Microchip are committed to continuously improving the code protection features of our products. Attempts to break Microchip's code protection feature may be a violation of the Digital Millennium Copyright Act. If such acts allow unauthorized access to your software or other copyrighted work, you may have a right to sue for relief under that Act.

Information contained in this publication regarding device applications and the like is provided only for your convenience and may be superseded by updates. It is your responsibility to ensure that your application meets with your specifications. MICROCHIP MAKES NO REPRESENTATIONS OR WARRANTIES OF ANY KIND WHETHER EXPRESS OR IMPLIED, WRITTEN OR ORAL, STATUTORY OR OTHERWISE, RELATED TO THE INFORMATION, INCLUDING BUT NOT LIMITED TO ITS CONDITION, QUALITY, PERFORMANCE, MERCHANTABILITY OR FITNESS FOR PURPOSE. Microchip disclaims all liability arising from this information and its use. Use of Microchip devices in life support and/or safety applications is entirely at the buyer's risk, and the buyer agrees to defend, indemnify and hold harmless Microchip from any and all damages, claims, suits, or expenses resulting from such use. No licenses are conveyed, implicitly or otherwise, under any Microchip intellectual property rights.

Trademarks

The Microchip name and logo, the Microchip logo, Accuron, dsPIC, KEELOQ, KEELOQ logo, microID, MPLAB, PIC, PICmicro, PICSTART, PRO MATE, rPIC and SmartShunt are registered trademarks of Microchip Technology Incorporated in the U.S.A. and other countries.

AmpLab, FilterLab, Linear Active Thermistor, Migratable Memory, MXDEV, MXLAB, SEEVAL, SmartSensor and The Embedded Control Solutions Company are registered trademarks of Microchip Technology Incorporated in the U.S.A.

Analog-for-the-Digital Age, Application Maestro, CodeGuard, dsPICDEM, dsPICDEM.net, dsPICworks, dsSPEAK, ECAN, ECONOMONITOR, FanSense, FlexROM, fuzzyLAB, In-Circuit Serial Programming, ICSP, ICEPIC, Mindi, MiWi, MPASM, MPLAB Certified logo, MPLIB, MPLINK, PICkit, PICDEM, PICDEM.net, PICLAB, PICtail, PowerCal, PowerInfo, PowerMate, PowerTool, REAL ICE, rLAB, Select Mode, Smart Serial, SmartTel, Total Endurance, UNI/O, WiperLock and ZENA are trademarks of Microchip Technology Incorporated in the U.S.A. and other countries.

SQTP is a service mark of Microchip Technology Incorporated in the U.S.A.

All other trademarks mentioned herein are property of their respective companies.

© 2007, Microchip Technology Incorporated, Printed in the U.S.A., All Rights Reserved.

 Printed on recycled paper.

**QUALITY MANAGEMENT SYSTEM
CERTIFIED BY DNV
== ISO/TS 16949:2002 ==**

Microchip received ISO/TS-16949:2002 certification for its worldwide headquarters, design and wafer fabrication facilities in Chandler and Tempe, Arizona; Gresham, Oregon and design centers in California and India. The Company's quality system processes and procedures are for its PIC® MCUs and dsPIC® DSCs, KEELOQ® code hopping devices, Serial EEPROMs, microperipherals, nonvolatile memory and analog products. In addition, Microchip's quality system for the design and manufacture of development systems is ISO 9001:2000 certified.



WORLDWIDE SALES AND SERVICE

AMERICAS

Corporate Office
2355 West Chandler Blvd.
Chandler, AZ 85224-6199
Tel: 480-792-7200
Fax: 480-792-7277
Technical Support:
<http://support.microchip.com>
Web Address:
www.microchip.com

Atlanta
Duluth, GA
Tel: 678-957-9614
Fax: 678-957-1455

Boston
Westborough, MA
Tel: 774-760-0087
Fax: 774-760-0088

Chicago
Itasca, IL
Tel: 630-285-0071
Fax: 630-285-0075

Dallas
Addison, TX
Tel: 972-818-7423
Fax: 972-818-2924

Detroit
Farmington Hills, MI
Tel: 248-538-2250
Fax: 248-538-2260

Kokomo
Kokomo, IN
Tel: 765-864-8360
Fax: 765-864-8387

Los Angeles
Mission Viejo, CA
Tel: 949-462-9523
Fax: 949-462-9608

Santa Clara
Santa Clara, CA
Tel: 408-961-6444
Fax: 408-961-6445

Toronto
Mississauga, Ontario,
Canada
Tel: 905-673-0699
Fax: 905-673-6509

ASIA/PACIFIC

Asia Pacific Office
Suites 3707-14, 37th Floor
Tower 6, The Gateway
Harbour City, Kowloon
Hong Kong
Tel: 852-2401-1200
Fax: 852-2401-3431

Australia - Sydney
Tel: 61-2-9868-6733
Fax: 61-2-9868-6755

China - Beijing
Tel: 86-10-8528-2100
Fax: 86-10-8528-2104

China - Chengdu
Tel: 86-28-8665-5511
Fax: 86-28-8665-7889

China - Fuzhou
Tel: 86-591-8750-3506
Fax: 86-591-8750-3521

China - Hong Kong SAR
Tel: 852-2401-1200
Fax: 852-2401-3431

China - Nanjing
Tel: 86-25-8473-2460
Fax: 86-25-8473-2470

China - Qingdao
Tel: 86-532-8502-7355
Fax: 86-532-8502-7205

China - Shanghai
Tel: 86-21-5407-5533
Fax: 86-21-5407-5066

China - Shenyang
Tel: 86-24-2334-2829
Fax: 86-24-2334-2393

China - Shenzhen
Tel: 86-755-8203-2660
Fax: 86-755-8203-1760

China - Shunde
Tel: 86-757-2839-5507
Fax: 86-757-2839-5571

China - Wuhan
Tel: 86-27-5980-5300
Fax: 86-27-5980-5118

China - Xian
Tel: 86-29-8833-7252
Fax: 86-29-8833-7256

ASIA/PACIFIC

India - Bangalore
Tel: 91-80-4182-8400
Fax: 91-80-4182-8422

India - New Delhi
Tel: 91-11-4160-8631
Fax: 91-11-4160-8632

India - Pune
Tel: 91-20-2566-1512
Fax: 91-20-2566-1513

Japan - Yokohama
Tel: 81-45-471- 6166
Fax: 81-45-471-6122

Korea - Daegu
Tel: 82-53-744-4301
Fax: 82-53-744-4302

Korea - Seoul
Tel: 82-2-554-7200
Fax: 82-2-558-5932 or
82-2-558-5934

Malaysia - Kuala Lumpur
Tel: 60-3-6201-9857
Fax: 60-3-6201-9859

Malaysia - Penang
Tel: 60-4-227-8870
Fax: 60-4-227-4068

Philippines - Manila
Tel: 63-2-634-9065
Fax: 63-2-634-9069

Singapore
Tel: 65-6334-8870
Fax: 65-6334-8850

Taiwan - Hsin Chu
Tel: 886-3-572-9526
Fax: 886-3-572-6459

Taiwan - Kaohsiung
Tel: 886-7-536-4818
Fax: 886-7-536-4803

Taiwan - Taipei
Tel: 886-2-2500-6610
Fax: 886-2-2508-0102

Thailand - Bangkok
Tel: 66-2-694-1351
Fax: 66-2-694-1350

EUROPE

Austria - Wels
Tel: 43-7242-2244-39
Fax: 43-7242-2244-393

Denmark - Copenhagen
Tel: 45-4450-2828
Fax: 45-4485-2829

France - Paris
Tel: 33-1-69-53-63-20
Fax: 33-1-69-30-90-79

Germany - Munich
Tel: 49-89-627-144-0
Fax: 49-89-627-144-44

Italy - Milan
Tel: 39-0331-742611
Fax: 39-0331-466781

Netherlands - Drunen
Tel: 31-416-690399
Fax: 31-416-690340

Spain - Madrid
Tel: 34-91-708-08-90
Fax: 34-91-708-08-91

UK - Wokingham
Tel: 44-118-921-5869
Fax: 44-118-921-5820